DRA-22. CHARACTERIZATION OF QUESTA DEBRIS FLOWS

G. Ayakwah, V.T. McLemore, A. Dickens, December 31, 2008, revised January 26, 2009
(reviewed by D. van Zyl)

1. STATEMENT OF THE PROBLEM

Can natural debris flows serve as mineralogical and physical proxies to long-term weathering of the Questa rock piles? What are the weathering products of the debris flows and how do they relate to the point load strength, slake durability index, and friction angle of the debris flows? Is the cementation of the debris flows similar to cementation found or expected to be found in the future within the Questa rock piles? Processes operating in the natural analogs share many similarities to those in the rock pile although certain aspects of the physical and chemical system are different.

2. PREVIOUS WORK

A debris flow is defined as a mixture of sediment and water that flows in a manner as if it was a continuous fluid driven by gravity, and it attains large mobility from the large void space saturated with water or slurry (Tamotsu, 2007). There has been extensive work on debris flows because of their disastrous nature, but very few debris flow studies include slake durability and point load strength tests. Dick and Shakoor (1995) stated that debris flows are the likely mode of failure in mudrocks of medium to low durability and tend to occur when developed regolith fails during heavy rains and wet periods. Viterbo (2007) studied the Goathill North (GHN) rock pile and stated that the slake durability and point load test values show that the rock fragments from the GHN rock pile are still quite strong even after being highly fractured and altered before being blasted, then emplaced in the pile and subsequently weathered. This DRA is focused on the Goat Hill debris flow (also known as the Goat Hill Gulch debris flow). More details are in Ayakwah et al. (2008).

Diagenesis is a broad term related to the chemical, physical, and biological changes affecting sediment after its initial deposition and during and after its lithification. Diagenesis does not include weathering or metamorphism of the sediment, but does include pedogenesis or the processes that form soils (Neuendorf et al., 2005). In terms of the Questa rock piles (man-made "sediment") and the debris flows (natural sediment), weathering and diagenetic processes overlap in time and space, especially in cementation of the rock-pile material. Cementation is the diagenetic process where sediments become lithified or consolidated or the binding-together of particles into hard, compacted rocks (Neuendorf et al., 2005). Cementation is important in the Questa study, because cementation could increase the slope stability of the rock piles in both the short (<100 years) and long term (>1000 years).

3. TECHNICAL APPROACH

A detailed mineralogical, chemical, and geotechnical study of a profile in the Goat Hill debris flow along Highway 38 documents the changes in weathering within this environment. This profile is constrained by ^{14}C dating of organic material found within the debris flow. Sampling procedures, descriptions and analytical procedures for soil profiles were used (URS Corporation, 2003; Smith and Beckie, 2003) and were the same as used elsewhere in the project (DRA-0, 6; Graf, 2008; McLemore et al., 2008). Geotechnical (slake durability, point load, moisture content, particle size analysis and laboratory direct shear) and geochemical (paste pH, TDS, conductivity,

scanning electron microprobe analysis, whole rock geochemistry, and petrographic analyses) testing were conducted to characterize the samples. Sampling procedures can be found in project SOPs and Ayakwah et al. (2008).

4. CONCEPTUAL MODEL

Debris flows near the Questa mine are naturally occurring sedimentary deposits that consist of similar lithologies as the Questa rock piles (hydrothermally altered andesite, rhyolite tuff, granitic intrusions). The debris flow was not deposited the same way as the Questa rock piles. Debris flows can be highly saturated during deposition, whereas the Questa rock piles were constructed of excavated rock material end-dumped onto steep mountain slopes and might not exhibit the exact characteristics. The debris flows were formed by a mixture of sediment and water that flow downhill in a natural drainage, whereas the rock piles were formed by end dumping of relatively dry, blasted rock material over the edge of a slope (McLemore et al., 2008). The sediment in the debris flow was weathered and eroded from the alteration scars and adjacent slopes, transported by water, deposited, and subjected to weathering and diagenesis after deposition. Since the stabilization of the debris flow, it has been subjected to similar weathering processes as the rock piles. The debris flows represent an intermediate age of weathering (1000 to 100,000 year scale, estimated) between the relatively young Questa rock piles (25-40 years) and the older alteration scars (>100,000 years) of the Red River valley. The debris flows are moderately to well cemented and the rock piles have similar cementation now and could become more cemented in the future. Appendix 1 in DRA-19 compares the similarities and differences between the Questa rock piles and analogs, including the debris flows.

5. STATUS OF COMPONENT INVESTIGATION

The results of the geochemical and geotechnical characterization for each of the debris flow samples are listed in Appendix 3, Table 3-1 to 3-3 and Ayakwah et al. (2008). A sample of wood was collected from within the debris flow approximately 40 ft below the top of the flow; the ^{14}C isotopic age of this sample is 4220 ± 40 years BP (Lueth et al., 2008). Figure 1 shows the location of the GHN debris flow and Figure 2 shows the location of sample points along the profile. Appendix 3 contains the geotechnical and geochemical results of the debris flow profile (Table 3-1 to 3-4 in Appendix 3) and Appendix 4 contains the descriptions of the individual samples (Table 4-1 Appendix 4). Figure 2-6 shows particle size distribution curves for the individual sample locations along the profile. The paste pH values are low (below pH 4).

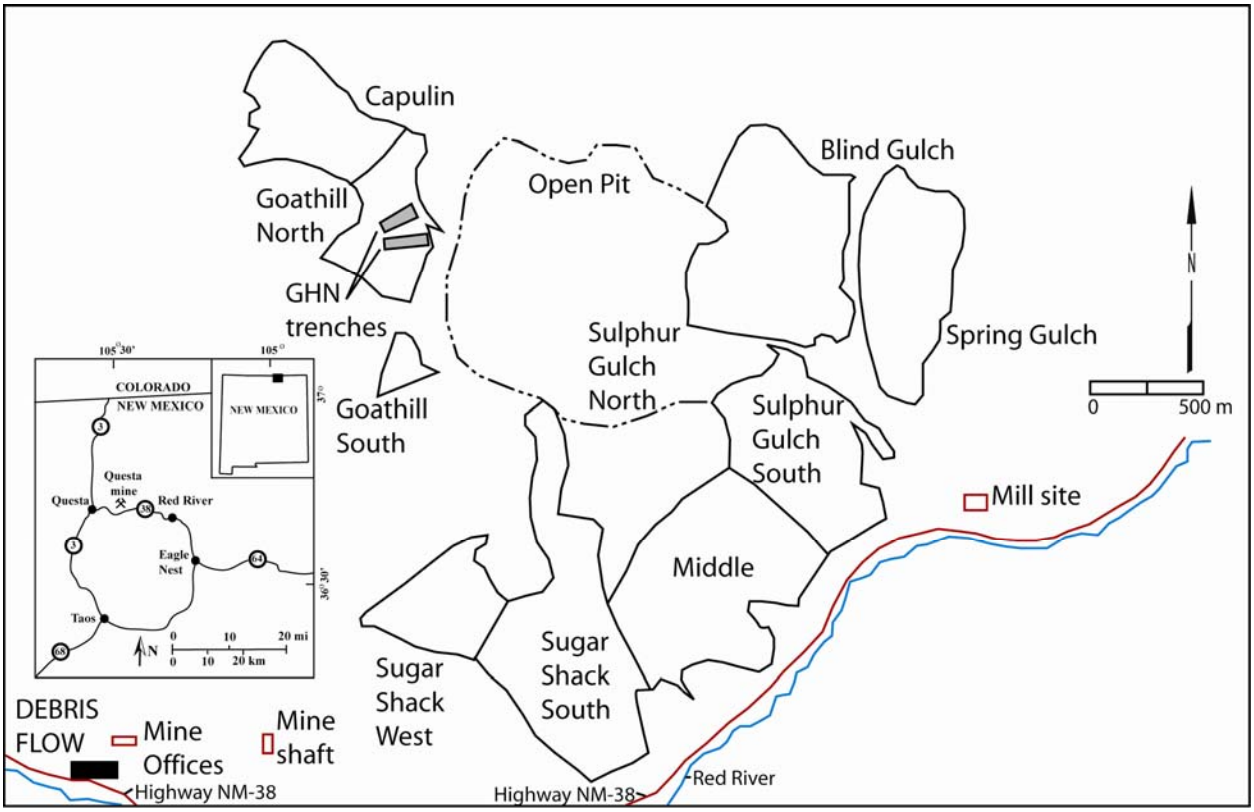

FIGURE 1. Location map of the Goat Hill debris flow.

FIGURE 2. Location of samples taken from the debris flow.

Although the samples along the profile have been hydrothermally altered, weathered and have clay minerals, the samples are still durable and strong. Samples from the profile exhibit high peak internal friction angles ranging from 38º to 51º, which can be attributed to the shape of the grains in the samples (subangular to very angular; Gutierrez, 2006; Gutierrez et al., 2008). Slake durability index ranged from 98 to 99% and point load strength index from 2.6 to 6 MPa with samples classified as extremely durable and high to very high strength, respectively, which

indicate that the samples from the debris flow are as strong as GHN (Gutierrez et al., 2008; Ayakwah et al., 2009). Plasticity Index ranged from 3 to 8%.

There is no observed clear trend of slake durability index, point load strength index, friction angle, percent gravel, density and water content with depth in the profile, which is probably related to the deposition of different material layers during different flow events that formed the debris flows (Figs. 1-1, 1-2; Appendix 1). The debris flow was formed by several different flood events over time. Two sample locations, MIN-GFA-0006 and MIN-GFA-0007 did not contain rock fragments suitable for testing for slake durability index and point load strength index. Figure 2-1 in Appendix 2 shows a weak positive correlation between slake durability index (%) and point load strength index (MPa), which implies that as slake durability increases, point load strength also increases. There is positive trend between paste pH, point load strength index, and slake durability index (Figure 2-3 in Appendix 2), which indicates that as point load and slake durability indices increase, paste pH also increases. There is a negative trend between friction angle and slake durability index (Fig. 2-1), which indicates that as point load and slake durability indices increases, friction angle decreases. However, there are not enough analyses to statistically call these correlations.

The plot of the S/SO_4 ratio with profile location indicates a relative decrease in the abundance of sulfate minerals towards the middle of the debris flow (Fig. 1-7 in Appendix 1). This could indicate rapid deposition of the material to prevent the oxidation of sulfide minerals. This also could be an indication of increase in sulfate mineralogy in the material before weathering, however the total S amount for this sample is slightly lower than the other samples from the debris flow.

The clay mineralogy from X-ray diffraction (XRD) analyses indicates that the samples from the weathering profile contain the same clay mineral groups as the Questa rock piles and the alteration scar samples. The samples from the debris flow contain illite, kaolinite, smectite, and minor chlorite (Fig. 3). The relative abundances of clay minerals do not vary significantly along the weathering profile. The XRD peak position of the smectite clay minerals indicate that the smectites contain only one structural water interlayer similar to the smectites found in the GHN rock pile (Donahue et al., 2008, 2009). Jarosite is present in all of the samples.

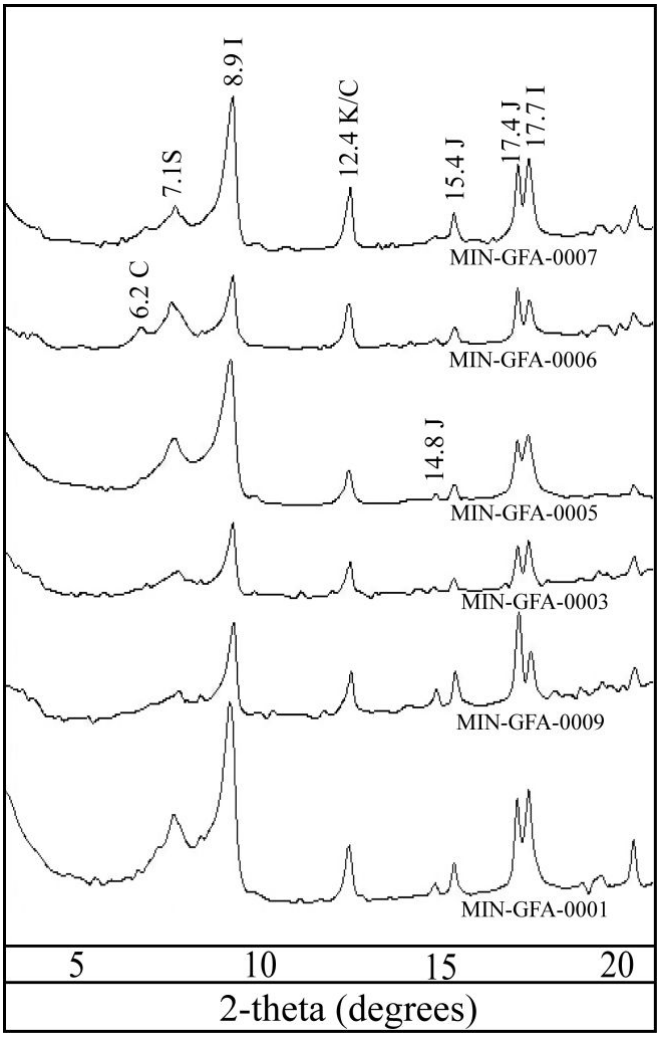

FIGURE 3. Clay mineralogy XRD scans for the debris flow weathering profile. I = illite, C = Chlorite, S = smectite, K = kaolinite, J = Jarosite.

Weathering and diagenic processes (especially cementation) have occurred in the debris flow, which is similar to that found in the rock piles. Figures 4 and 5 shows the similarity in texture and mineralogy of the cementation found in the debris flow with the GHN rock piles.

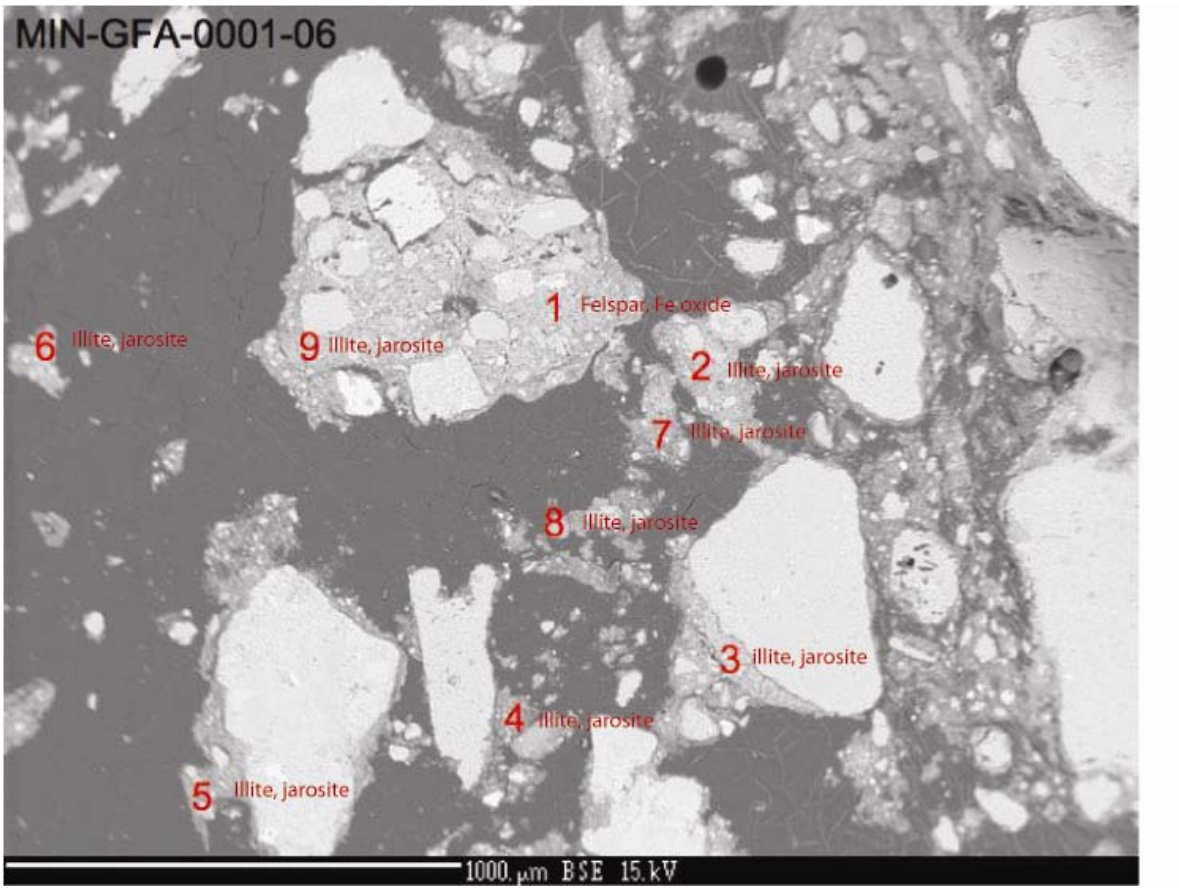

FIGURE 4. Backscattered electron microprobe image showing hydrothermally-altered phenocrysts and well cemented grains within MIN-GFA-0001 sample from the rock pile. The numbered points represent points for mineral chemistry. Illite, jarosite and Fe oxide crystals are cementing the rock fragments. The cementation is similar in chemistry and texture as that found in the GHN rock pile (Fig. 5).

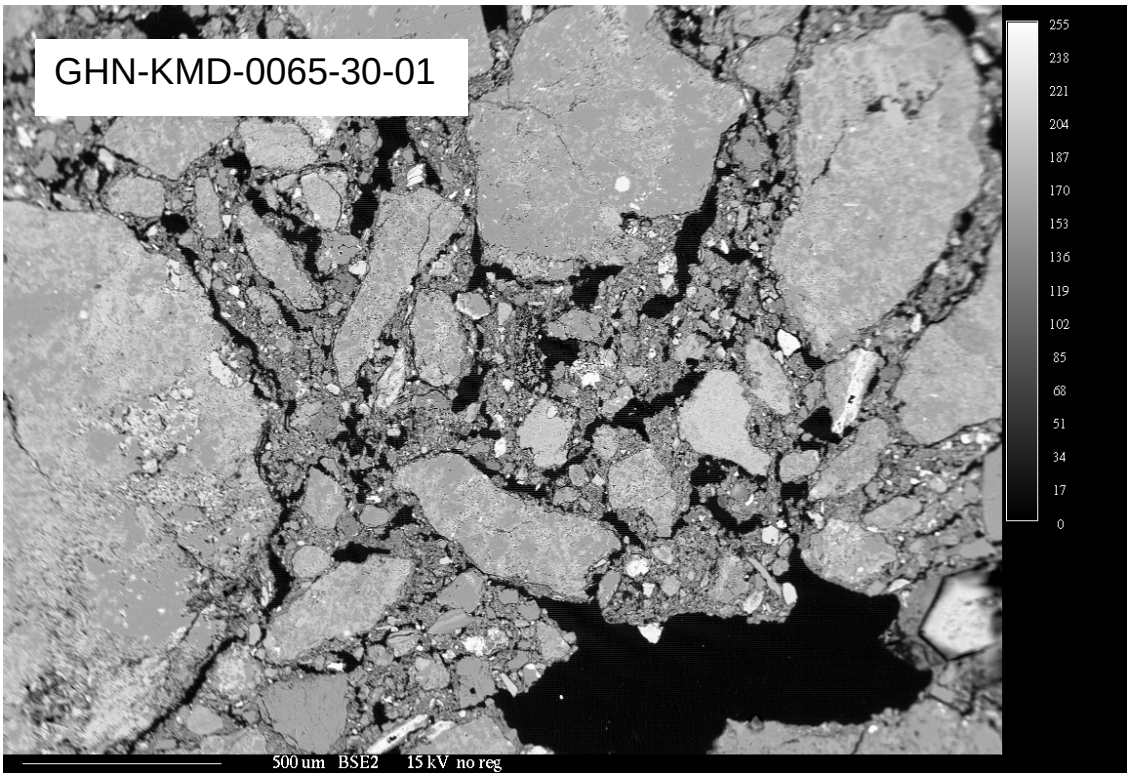

FIGURE 5. Backscattered electron image (BSE) showing soil sample showing rock fragment and associated fine-grained matrix material. Note the similarity in texture of the cementation of rock fragments in this image compared to the image in Figure 4. The fine-grained matrix consists of clay minerals and gypsum.

6. RELIABILITY ANALYSIS

Samples collected are complete, comparable, and representative of the defined population at the defined scale. Precision and accuracy are measured differently for each field and laboratory analysis (parameter), and is explained in the project reports, SOPs and DRAs and described in more detail in McLemore and Frey (2008). Most laboratory analyses depend upon certified reference standards and duplicate and triplicate analyses as defined in the project SOPs. The sampling and analysis plans for each segment of the field program and the control of accuracy and precision as defined in the SOPs, provides a large high-quality set of observations and measurements that are adequate to support the interpretations and conclusions of the various technical studies documented in this DRA. It is assumed that the large rock fragments (40 to 60 g, approximately 4-10 cm in size) tested have similar strength as the small rock fragments within the various rock piles and analog sites, including the debris flow.

The scientific inferences in this phase of the project include:

- Processes operating in the debris flow are the same as those for the rock piles
- Rock pile materials will become more like debris flows with time.

The technical and data uncertainties include:

- Only one weathering profile in debris flow was studied.
- Hydrologic and geologic frameworks are different between the debris flows and rock piles.

- Absolute time calibration–geochronological dating only assigns a bracket of ages but the range of ages is so large (up to 4000 years in the debris flow), the impact of age uncertainties is small with in the decision-making range of the study (100 to 1000 years).

Resolution of discrepancies in data and uncertainties include:

- The use of SOPs and QA procedures ensures that sample-to-sample comparisons for given analytical methods are reliable.
- Even though the same processes have been operating on equivalent starting materials for 300k-1.8Ma, the mineralogical outcomes in the very old deposits does not show evidence of mineralogical transformations (particularly quantitative formation of clay minerals) that would lead to decreasing shear strength.

7. CONCLUSION OF THE COMPONENT

The Goat Hill debris flow is not a typical residual weathering profile, because there are no clear trends within the debris flow profile to indicate an increase in weathering with depth in the profile. Instead the debris flow consists of several different flow events. However, weathering and diagenic processes (especially cementation) have occurred in the debris flow, which are similar to those found in the rock piles. Cementation is similar in texture and mineralogy in the debris flow and the GHN rock piles. As diagenesis progresses in the rock piles, it is likely that similar cementation could increase.

The results of the geochemical characterization indicate that the samples collected from the debris flow are similar to each other and to the Questa rock piles (McLemore et al., 2008), but do not show trends of decreasing weathering from the top of the profile to the bottom. The paste pH values for all of the samples range from 3.2 to 3.9, however there is no clear trend with depth (Figs. 1-2-to 1-8 in Appendix 1). The sulfide to sulfate ratio does not indicate an increase in sulfate minerals with increasing depth (Figure 1-7 in Appendix 1). The clay mineralogy from X-ray diffraction (XRD) analyses indicates that the samples from the weathering profile contain the same clay mineral groups as the Questa rock piles and the alteration scar samples.

The results of the geotechnical testing indicate there is no clear trend of decreasing strength with increasing depth for the samples from the debris flow profile. The point load and slake durability values for the debris flow profile are within the ranges found in the Questa rock piles (Table 4-2 in Appendix 4) and at the top of the debris flow in situ tests were conducted (Boakye, 2008). The geotechnical parameters do not increase in strength with depth (Figure 1-2 in Appendix 1). The moisture content of the samples from within the profile range between 3.6 and 5.4% and are similar to the moisture contents of the Questa rock piles (Table 4-2 in Appendix 4). The moisture content does not appear to have a trend with depth (Figure 1-2 in Appendix 1). The low percentage of fines in the samples could be the result of clay-size particles remaining as larger silt- to sand-sized aggregates during the dry sieving process. The sample with the highest peak friction angle (MIN-GFA-0001) also has the highest percentage of gravel, contained angular rock fragments, and highest dry density (Table 3-1 in Appendix 3). These factors combined are most likely attributed to the high friction angle of these samples. The slake durability and point load indices indicate that the debris flow materials are as strong as the other Questa materials (Table 4-2 in Appendix 4).

The debris flows are similar to the Questa rock piles in DRA 19 and also Table 4-2 in Appendix 3. The profile studied is not a weathered profile. There is no systematic variation in the

composition of the samples collected from the profile, indicating that the debris flow was formed in several different events with slightly different sources (DRA 19).

However, the debris flows are moderately to well cemented. The cementation is similar to that found in the Questa rock piles and is formed, in part, by oxidation of sulfide minerals producing sulfates and iron oxides. The debris flows are well cemented even below the surface and at the in-situ test locations at the top of he profile (DRA-47, McLemore and Dickens, 2008). Portions of the Questa rock piles are poorly cemented or have no cementation, but other portions, especially the outer layers are moderately to well cemented (see McLemore et al., 2008; Boakye, 2008; DRA-6, 8, 47). This cementation is formed in part through the breakdown of the rock fragments during erosion and re-deposition releasing hydrothermal clay minerals that then form cementing agents in the debris flow. These clay minerals are pre-debris flow hydrothermal clays and are not formed after deposition of the debris flow. Also the oxidation of pyrite forms jarosite, gypsum and iron oxides.

Distribution of sulfide and sulfate minerals suggests an open-system behavior (i.e. movement of sulfate within the debris flow). No trends in silicate minerals (including clays) suggest that no new silicate minerals are forming during weathering, similar to interpretations found in the Questa rock piles (McLemore et al., 2008) and alteration scars (Graf, 2008).

8. REFERENCES

Ayakwah, G., McLemore, V.T., and Dickens, A., 2008, Characterization of Questa debris flows: unpublished report to Chevron Mining Corporation, Task B1.4.

Ayakwah, G., McLemore, V.T., Fakhimi, A., Viterbo, V.C., and Dickens, A.K., 2009, Effects of weathering and alteration on point load and slake durability indices of Questa mine materials, New Mexico: Society of Mining, Metallurgy and Exploration Annual Convention, preprint Preprint 09-19.

Boakye, K., 2008, Large In Situ Direct Shear Tests on Rock Piles At The Questa Mine, Taos County, New Mexico: M.S. thesis, New Mexico Institute of Mining and Technology, Socorro, http://geoinfo.nmt.edu/staff/mclemore/Molycorppapers.htm.

Dick, J.C. and Shakoor, A. 1995, Characterizing durability of mud rocks for slope stability purposes: Geological Society America, Reviews in Engineering Geology, v. X, p. 121-130.

Donahue, K.M., Dunbar, N.W., Heizler, L., and McLemore, V.T., 2008, Origins of clay minerals in the Molycorp Mine Goathill North Rock pile, Questa NM: revised unpublished report to Chevron Mining Corporation.

Donahue, K.M., Dunbar, N.W., and McLemore, V.T., 2009, Clay mineralogy of the Goathill North rock pile, Questa mine, Taos County, NM: Origins and indications of in-situ weathering: Society of Mining, Metallurgy and Exploration Annual Convention, Denver, Feb 2009.

Graf, G., 2008, Mineralogical and geochemical changes associated with sulfide and silicate weathering in natural alteration scars, Taos County, New Mexico: M.S. thesis, New Mexico Institute of Mining and Technology, Socorro, 193 p., http://geoinfo.nmt.edu/staff/mclemore/Molycorppapers.htm, accessed April 28, 2008.

Gutierrez, L.A.F., 2006, The influence of mineralogy, chemistry and physical engineering properties on shear strength parameters of the Goathill North rock pile material, Questa

Molybdenum mine, New Mexico: M.S. thesis, New Mexico Institute of Mining and Technology, Socorro, 201 p., http://geoinfo.nmt.edu/staff/mclemore/Molycorppapers.htm, accessed December 06, 2007.

Gutierrez, L.A.F., Viterbo, V.C., McLemore, V.T., and Aimone-Martin, C.T., 2008, Geotechnical and Geomechanical Characterisation of the Goathill North Rock Pile at the Questa Molybdenum Mine, New Mexico, USA; *in* Fourie, A., ed., First International Seminar on the Management of Rock Dumps, Stockpiles and Heap Leach Pads: The Australian Centre for Geomechanics, University of Western Australia, p. 19-32.

Lueth, V.W., Samuels, K.E., and Campbell, A.R., 2008, Final Report (Phase II) on the Geochronological dating of Red River area alteration scars and debris flows: unpublished report to Chevron Mining Corporation, Task 1.13.5, 18 p.

McLemore, V.T., Boakye, K., Campbell, A., Donahue, K., Dunbar, N., Gutierrez, L. Heizler, L., Lynn, R., Lueth, V., Osantowski, E., Phillips, E., Shannon, H., Smith, M. Tachie-Menson, S., van Dam, R., Viterbo, V.C., Walsh, P., and Wilson, G.W., 2008, Characterization of Goathill North Rock Pile: revised unpublished report to Molycorp, Tasks: 1.3.3, 1.3.4, 1.4.2, 1.4.3, 1.11.1.3, 1.11.1.4, 1.11.2.3, B1.1.1, B1.3.2.

McLemore, V.T. and Dickens, A., 2008, Petrographic Analysis, Mineralogy, and Chemistry of Samples Analyzed by In-Situ Direct Shear Methods, Questa, New Mexico: report to Chevron, Task B1.

McLemore, V.T. and Frey, B., 2008, Quality control and quality assurance report: unpublished report to Chevron, Task B1.

McLemore, V., Sweeney, D., Dunbar, N., Heizler, L. and Phillips, E., 2009, Determining quantitative mineralogy using a combination of petrographic techniques, whole rock chemistry, and MODAN: Society of Mining, Metallurgy and Exploration Annual Convention, preprint 09-20, 19 p.

Neuendorf, K.K.E., Mehl, J.P., Jr., and Jackson, J.A., 2005, Glossary of Geology: American Geological Institute, 5th ed., Alexandria, Virginia, 779 p.

Smith, L. and Beckie, R., 2003, Hydrologic and geochemical transport processes in mine waste rock: Mineralogical Association of Canada, Short Course Series, v. 21, p. 51-72.

Tamotsu, T. 2007, Debris flow mechanics, prediction and countermeasures: Balkema-Proceedings-Engineering, p 6.

URS Corporation, 2003, Mine rock pile erosion and stability evaluations, Questa mine: Unpublished Report to Molycorp, Inc. 4 volumes.

Viterbo, V., 2007, Effect of premining hydrothermal alteration processes and postmining weathering on rock engineering properties of Goathill north rock pile at the Questa Mine, Taos, New Mexico: M. S. thesis, New Mexico Institute of Mining and Technology, Socorro, NM, 209 p., http://geoinfo.nmt.edu/staff/mclemore/Molycorppapers.htm, accessed March 10, 2008.

9. TECHNICAL APPENDICES

Ayakwah, G., McLemore, V.T., and Dickens, A., 2008, Characterization of Questa debris flows: unpublished report to Chevron Mining Corporation, Task B1.4.

APPENDIX 1. Geochemical, mineralogical and geotechnical changes plots along the profile.

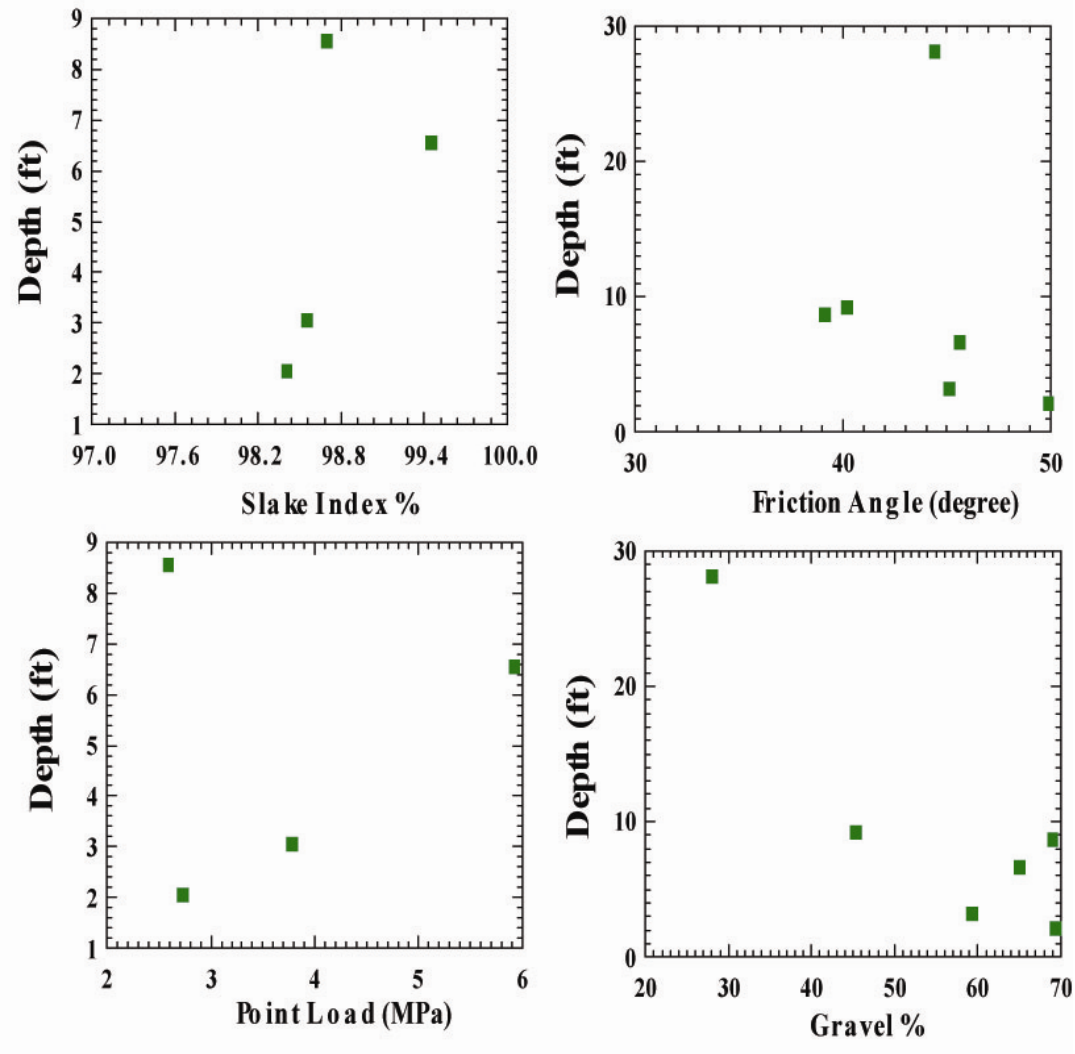

FIGURE 1-1. Slake index, friction angle, point load index and percent gravel with depth from the base of the debris flow profile. No observed trend of parameters with depth.

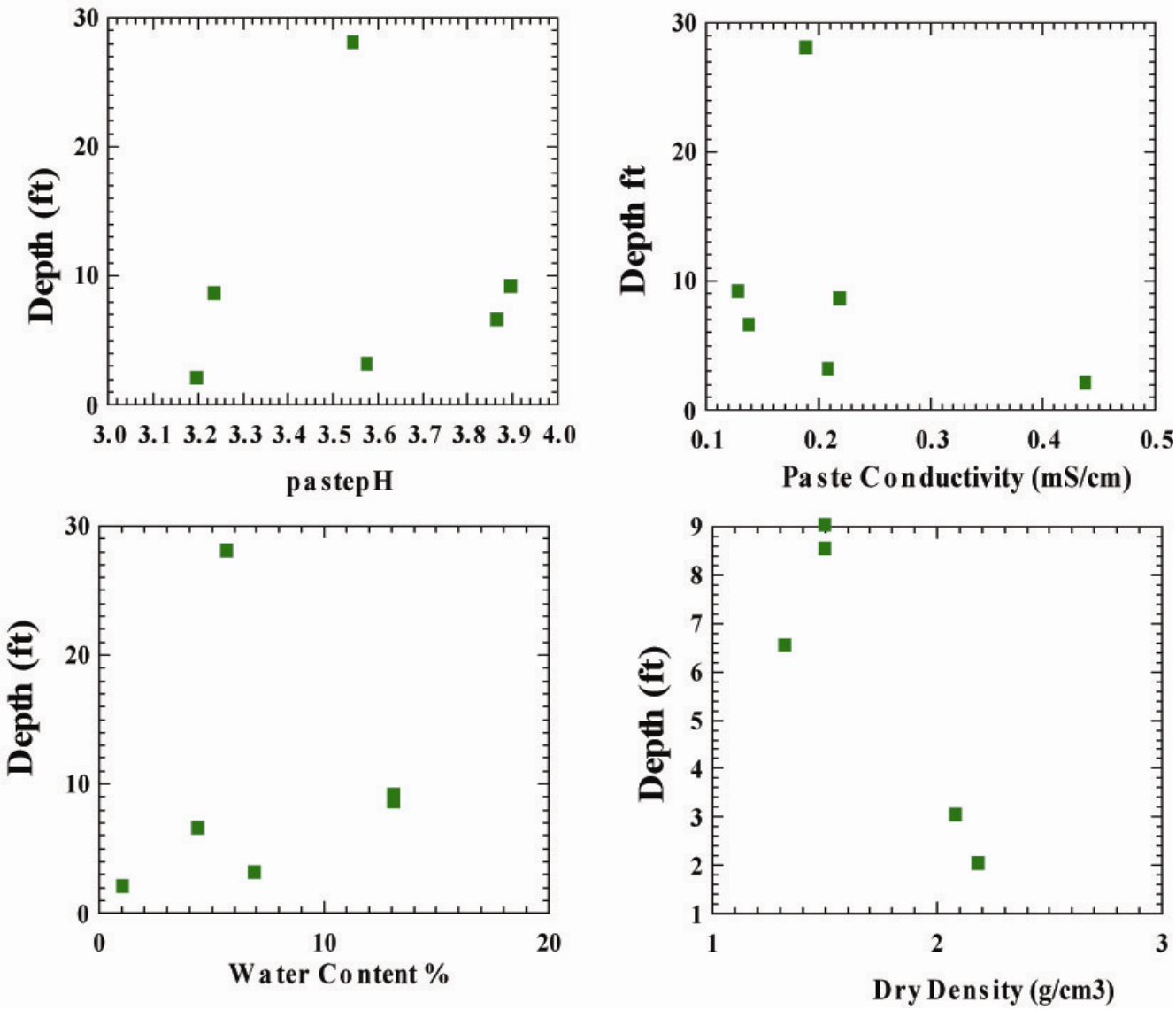

FIGURE 1-2. Paste pH, paste conductivity, water content and dry density with depth from the base of the debris flow profile. No clear trend was observed between the parameters and depth.

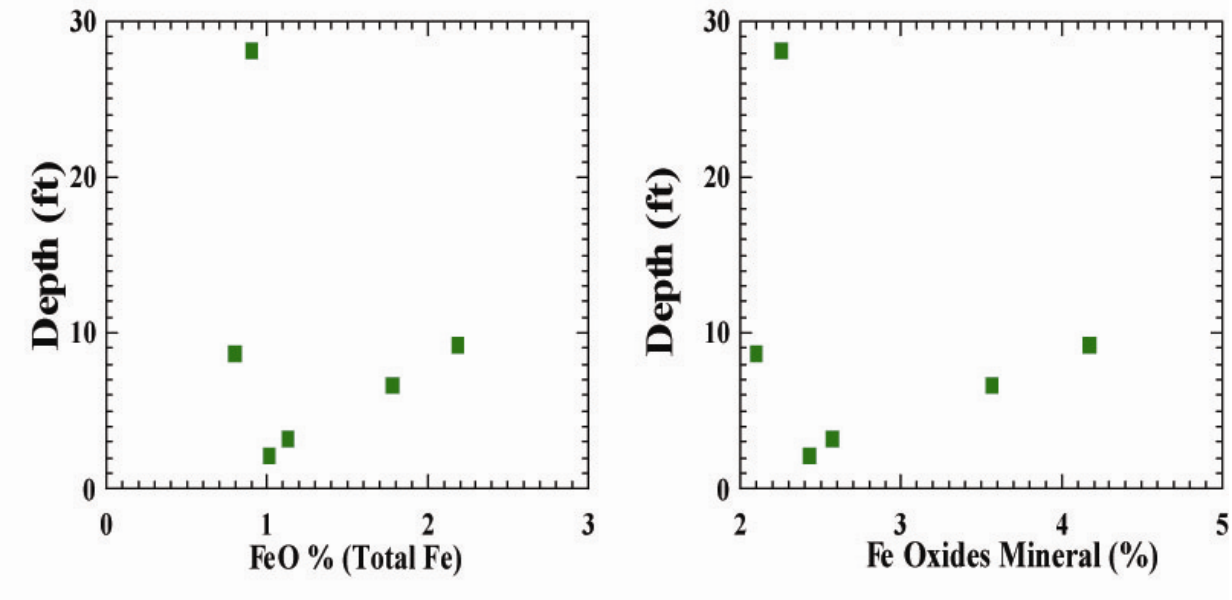

FIGURE 1-3. Percent of FeO and Fe oxide minerals with depth from the base of the debris flow profile**.** No clear trend of parameters with profile.

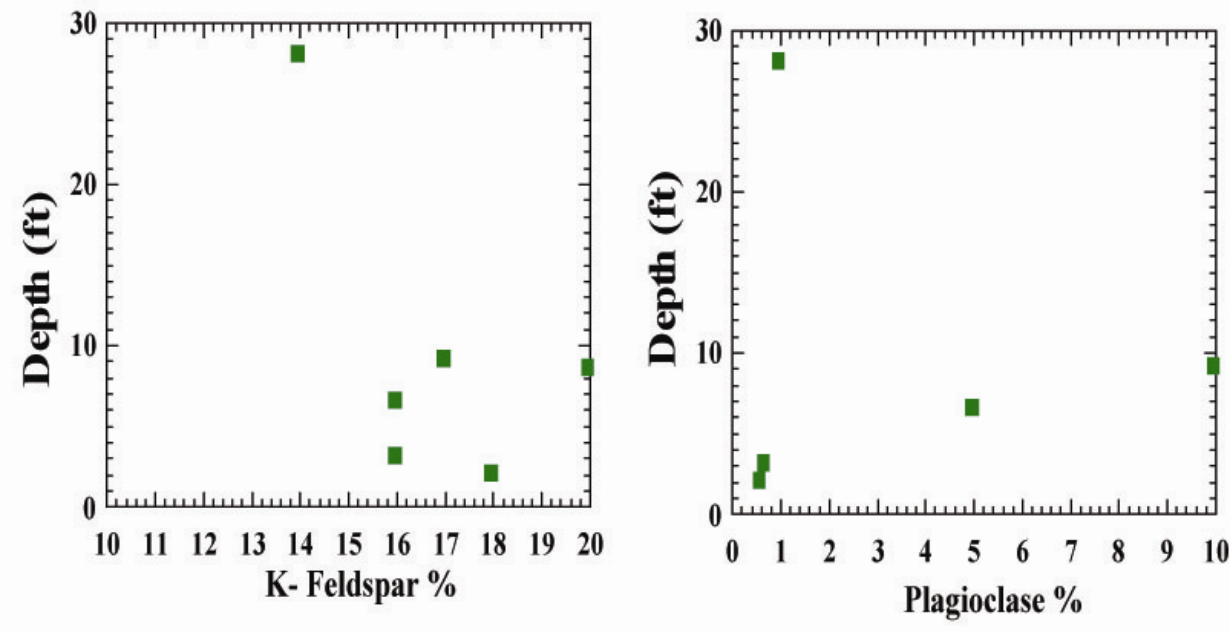

FIGURE 1-4. Total feldspar (K-feldspar+plagioclase) with depth from the base of the debris flow profile. No clear trend of parameters with profile.

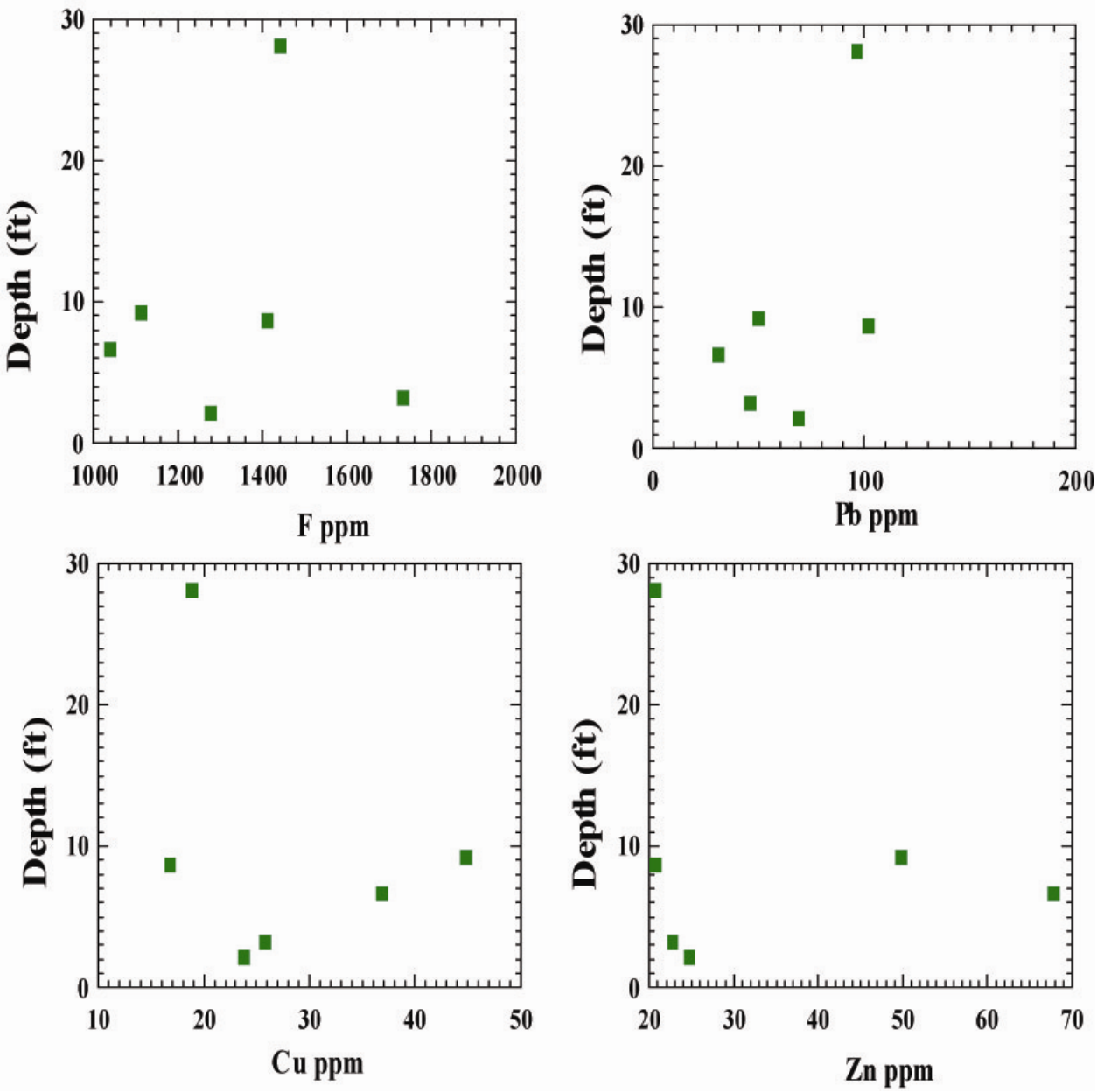

FIGURE 1-5. Selected trace elements with depth from the base of the debris flow profile. No clear trend of trace elements with profile.

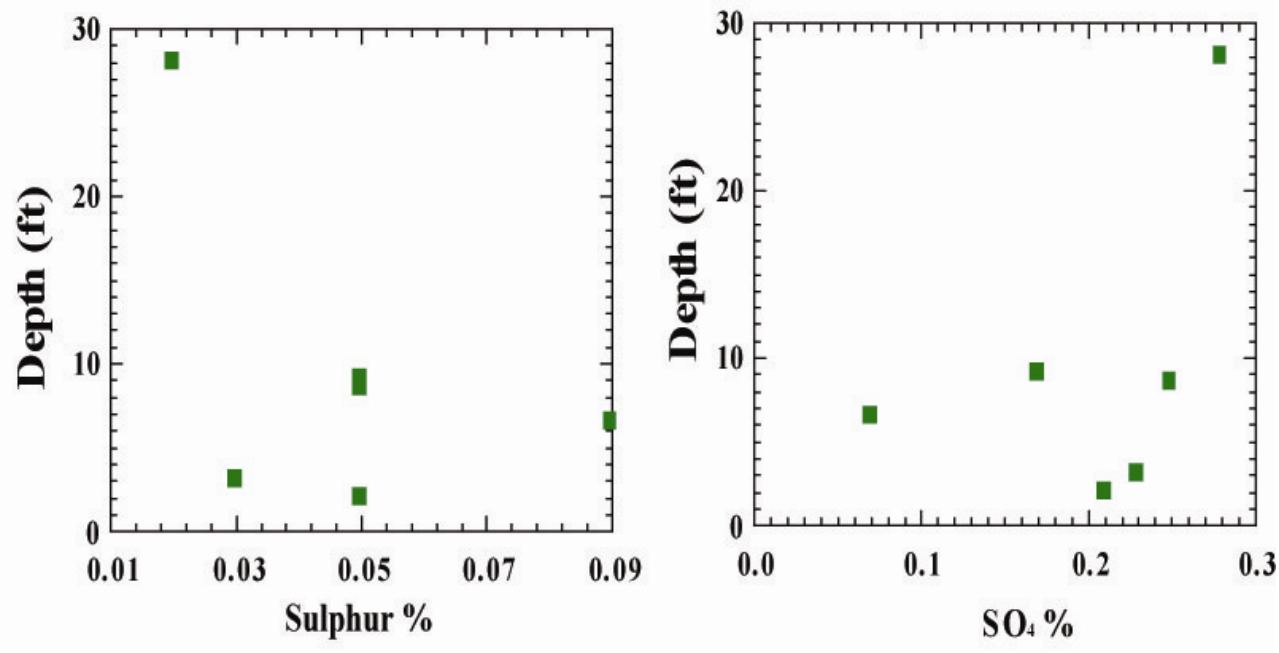

FIGURE 1-6. Sulfur and SO_4 with depth from the base of the debris flow profile**.** No clear trend of parameters with profile.

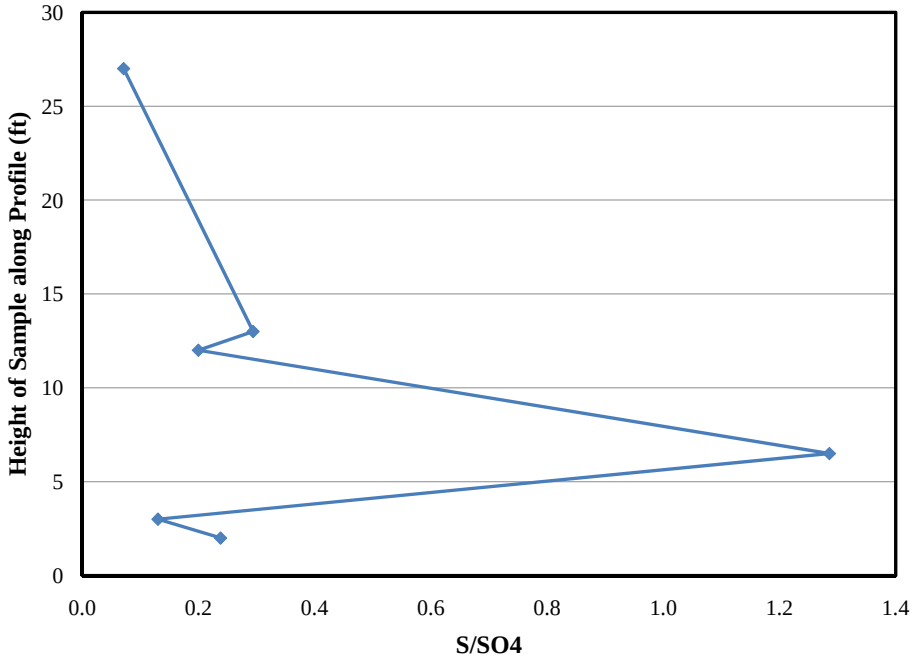

FIGURE 1-7. Sulfur/Sulfate ratio with depth from the base of the debris flow profile. No clear trend of sulfur/sulfate with profile.

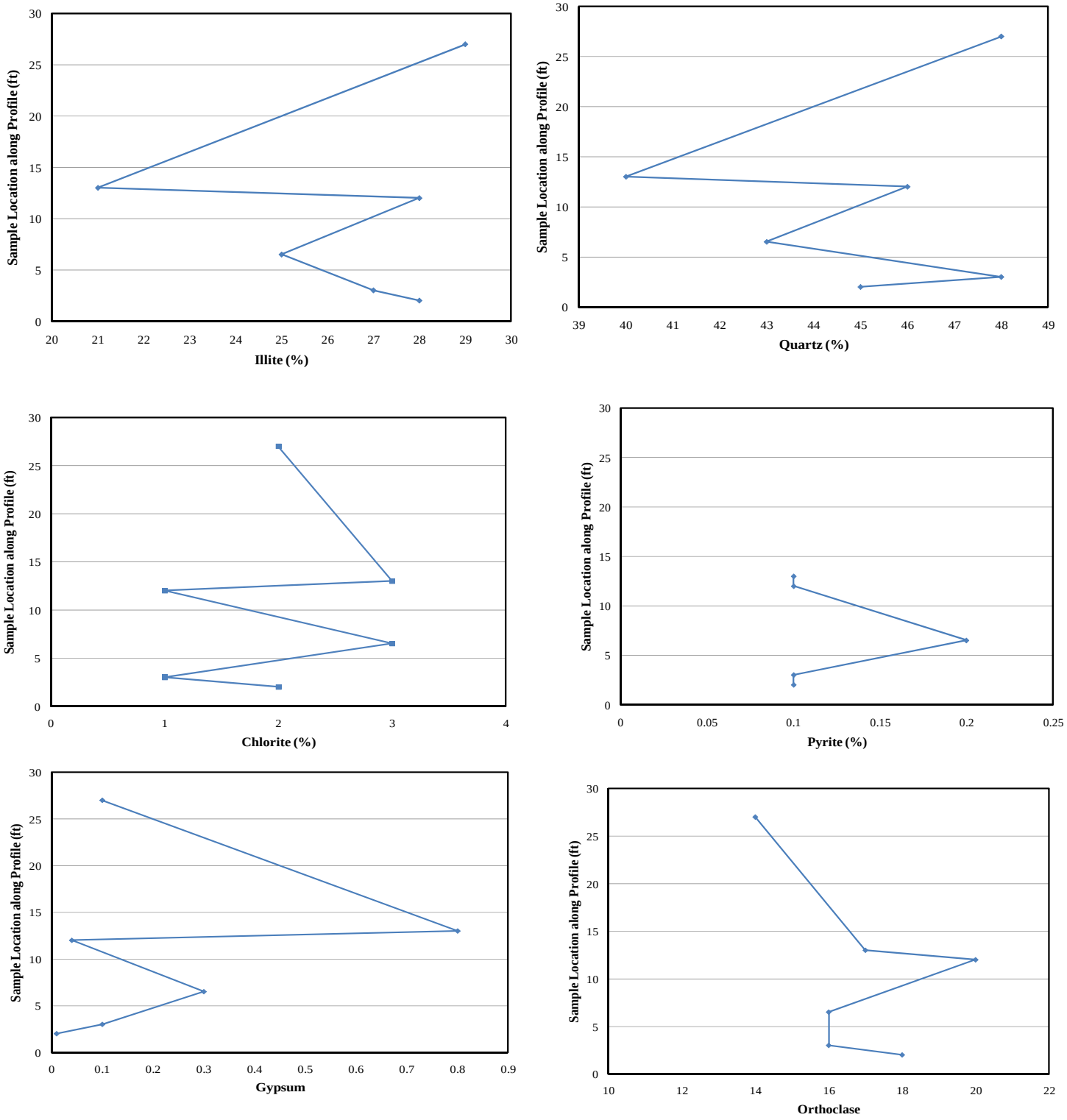

FIGURE 1-8. Geochemical and mineralogical parameters on the X-axis and sample location along the profile from base to top on the y-axis. No clear trend of parameters along the profile.

APPENDIX 2. Scatter plots of geochemical and geotechnical parameters

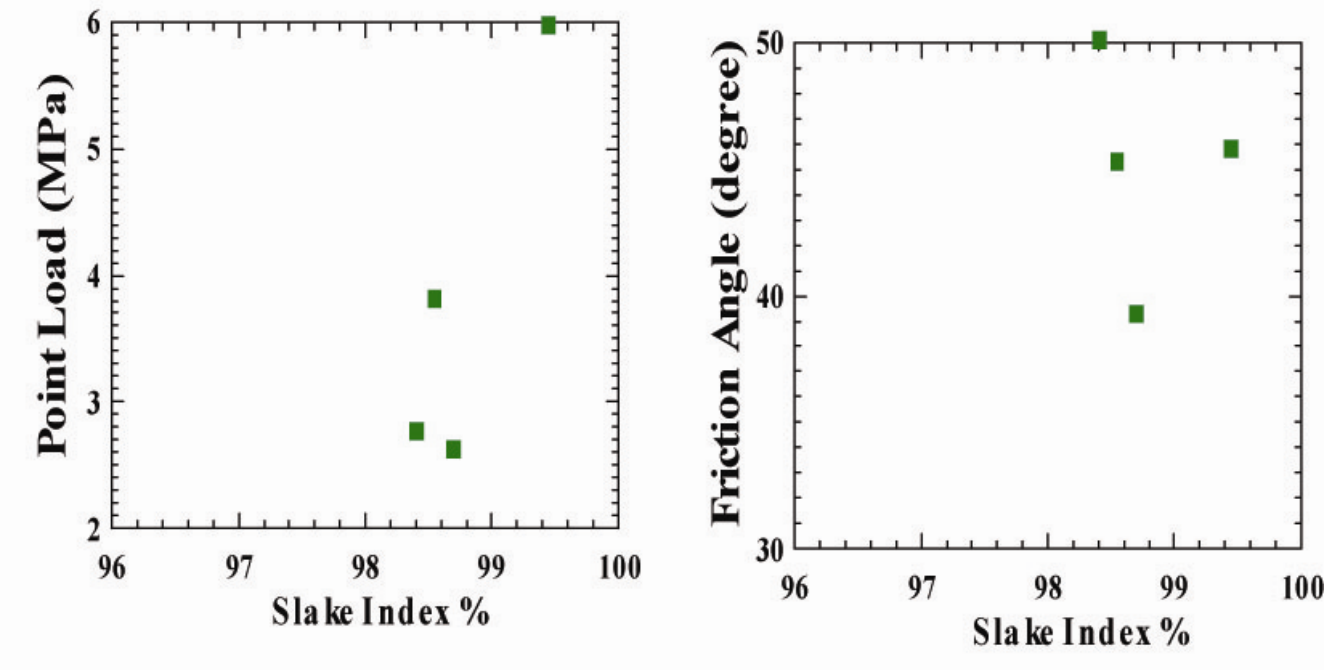

FIGURE 2-1. Slake durability indices (%) plotted against point load index and friction angle. Point load shows a positive trend as slake durability index increases. Point load index also increases as slake durability index increases. There is a weak negative trend between slake durability index and friction angle. However, there are not enough analyses to statistically call these correlations.

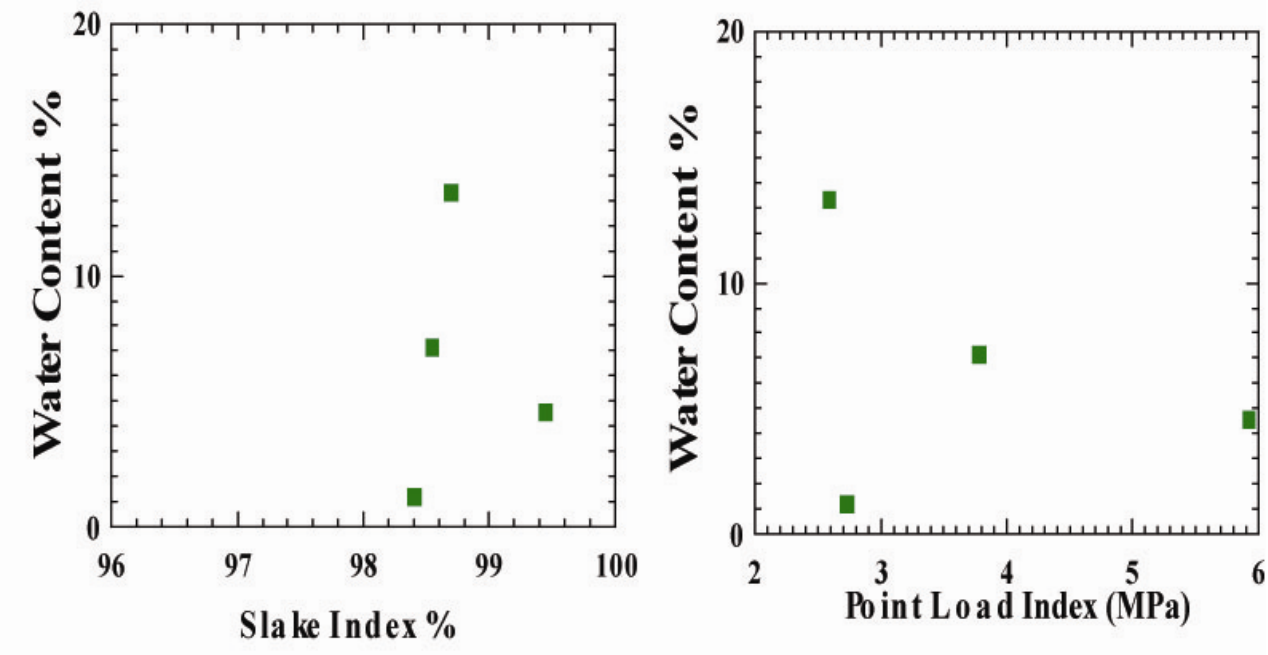

FIGURE 2-2. Slake durability indices (%) and point load index with water content showing a weak negative trend; as water content increases slake durability index and point load index decreases.

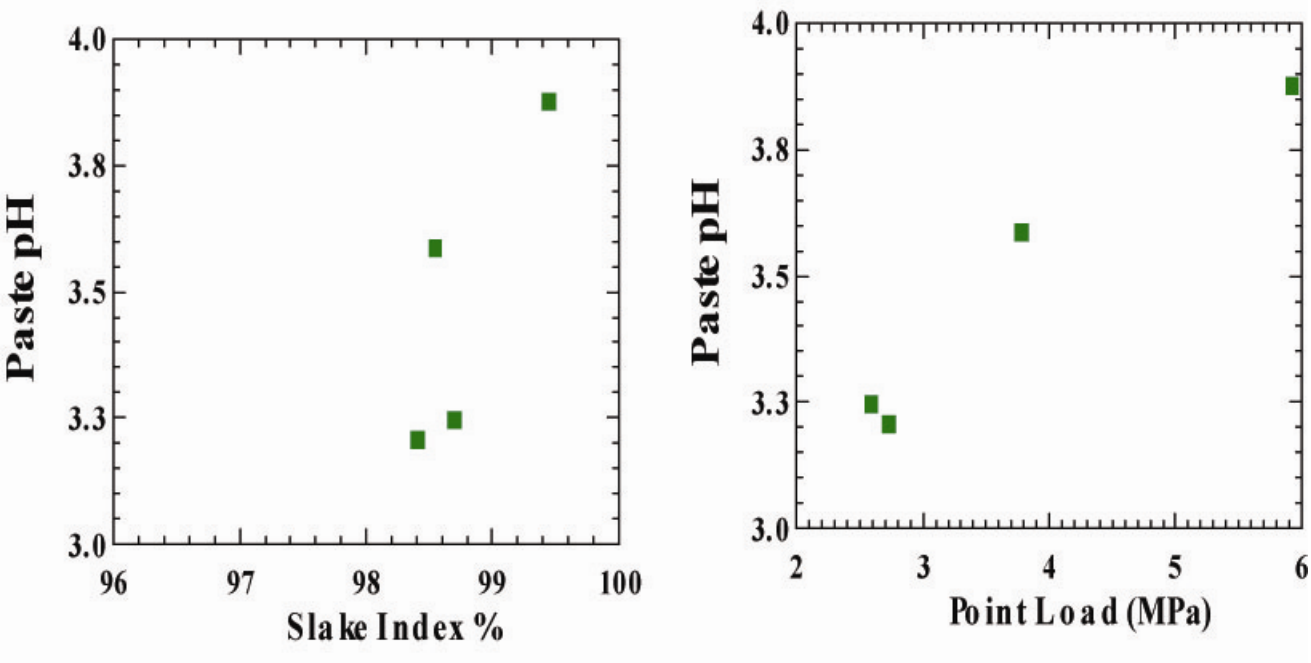

FIGURE 2-3. Slake index and point load index with paste pH each indicating a positive trend as paste pH increases slake durability index and point load index increases.

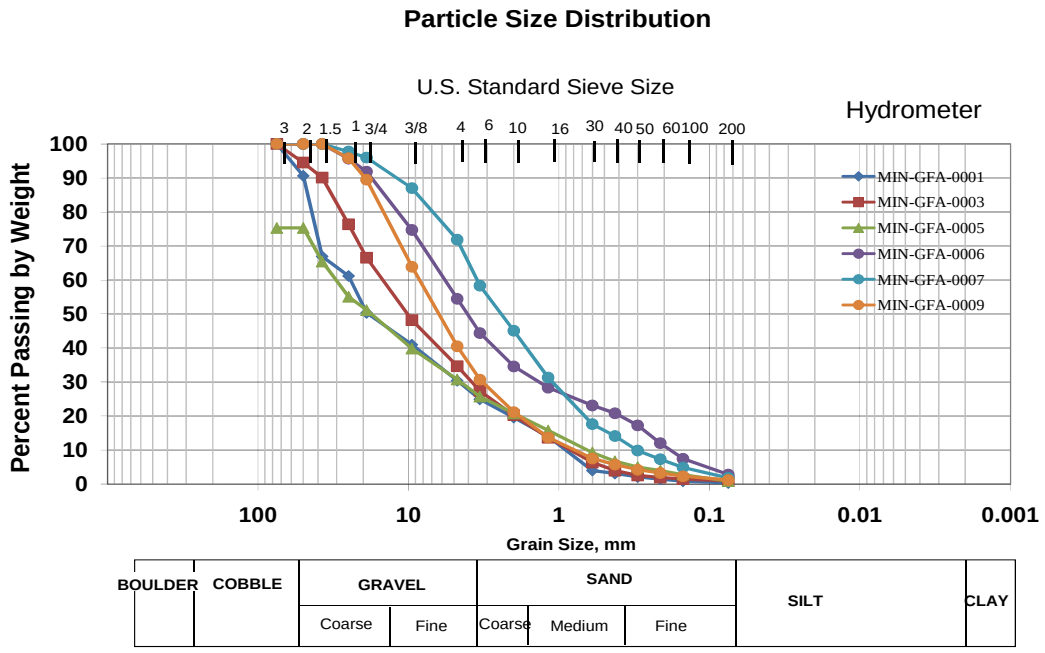

FIGURE 2-4. Particle size distribution curves of the six samples along the profile

APPENDIX 3. Summary laboratory results of the debris flow profile samples.

TABLE 3-1. Geological and geotechnical parameters of samples collected from the debris flow profile. Samples MIN-GFA-0006 and MIN-GFA-0007 did not contain rock fragments, but were mostly soil materials and therefore, point load and slake durability tests were not performed on them.

Sample	MIN-GFA-0001	MIN-GFA-0003	MIN-GFA-0005	MIN-GFA-0006	MIN-GFA-0007	MIN-GFA-0009
Paste pH	3.2	03.87	3.24	3.9	3.55	3.58
Paste Conductivity (mS/cm)	0.44	0.14	0.22	0.13	0.19	0.21
Water Content %	4.46	4.69	4.12	3.68	5.44	5.00
Geotechnical Parameters						
Slake Index %	98.42	99.46	98.71			98.57
Point Load MPa	2.80	6.00	2.6			3.60
Dry Density g/cm^3	2.19	1.33	1.51	1.51	1.17	2.09
Friction Angle (degrees)	50.00	45.70	39.20	40.30	44.50	45.20
Residual Friction Angle (degrees)	37.80	33.80	34.90	34.80	36.00	35.50
Atterberg Limits						

Sample	MIN-GFA-0001	MIN-GFA-0003	MIN-GFA-0005	MIN-GFA-0006	MIN-GFA-0007	MIN-GFA-0009
Liquid Limit	24.84		28.24		25.50	24.64
Plastic Limit	18.68		19.32		18.77	21.59
Plastic Index	6.16		8.92		6.77	3.05
Particle Size Distribution						
Gravel %	69.60	65.34	69.25	45.53	28.15	59.50
Sand %	30.07	33.74	29.88	51.66	70.01	39.28
Silt %	0.30	0.92	0.87	2.81	1.84	1.22
Clay %						
Fines %	0.32	0.92	0.87	2.81	1.84	1.22
D10 %	0.90	0.86	0.66	0.20	0.30	0.80
D30 %	4.80	3.95	4.50	1.40	1.10	3.20
D50 %	20.00	10.00	18.00	4.00		6.20
D60 %	23.00	15.00	30.00	5.80	3.60	8.60

TABLE 3-2. Chemical composition of samples collected from debris flow profile. Oxides are in weight percent and trace elements are in parts per million.

Sample	MIN-GFA-0001	MIN-GFA-0003	MIN-GFA-0005	MIN-GFA-0006	MIN-GFA-0007	MIN-GFA-0009
SiO_2	72.65	70.88	73.70	70.03	73.95	74.70
TiO_2	0.50	0.46	0.39	0.51	0.41	0.40
Al_2O_3	13.17	12.98	13.2	12.97	12.92	12.50
FeOT	2.22	3.26	1.92	3.81	2.06	2
MnO	0.22	0.39	0.02	0.04	0.02	0.02
MgO	0.79	1.23	0.68	1.27	0.67	0.6
CaO	0.1	0.71	0.02	0.56	0.05	0.06
Na_2O	0.62	1.07	0.46	1.65	0.58	0.57
K_2O	4.31	3.53	4.19	3.41	4.00	4.03
P_2O_5	0.10	0.18	0.09	0.19	0.11	0.13
S	0.05	0.09	0.05	0.05	0.02	0.03
SO_4	0.21	0.07	0.25	0.17	0.28	0.23
S/SO_4	0.24	1.29	0.20	0.29	0.07	0.13
C	0.02	0.03	0.01	0.08	0.04	0.03
LOI	3.46	2.91	3.68	3.95	3.80	3.42
Total	98.65	98.11	98.86	99.06	99.12	99.30
Ba	642	822	613	871	666	591
Rb	149	104	149	104	134	137
Sr	133	280	138	265	140	145
Pb	70	32	103	51	98	47
Th	13	8	12	8	13	11
U	5	6	4.5	4.00	5.00	5.00
Zr	215	172	240.50	189.00	226.00	213.00
Nb	24.00	16.90	25.50	16.20	24.10	24.00
Y	32.00	23.00	40.00	21.00	35.00	33.00
Sc	5.00	6.00	4.00	7.00	5.00	5.00
V	61	62	46	73	46	44

Sample	MIN-GFA-0001	MIN-GFA-0003	MIN-GFA-0005	MIN-GFA-0006	MIN-GFA-0007	MIN-GFA-0009
Ni	5	14	1	12	1	1
Cu	24	37	17	45	19	26
Zn	25	68	21	50	21	23
Ga	20	17	22		21	19
Cr	42	43	27	53	29	30
F	1281	1045	1416	1116	1448	1737
La	47	29	50	34	46	46
Ce	95	57	98	63	98	91
Nd	41	25	41.5	24	41	37

TABLE 3-3. Mineral composition of samples collected from debris flow profile, in weight percent (as determined by bulk mineralogy method from the modified ModAn method, McLemore et al., 2009). QSP=quartz, pyrite, sericite alteration.

Sample	MIN-GFA-0001	MIN-GFA-0003	MIN-GFA-0005	MIN-GFA-0006	MIN-GFA-0007	MIN-GFA-0009
SWI	3			3	3	3
illite	28	25	28	21	29	27
chlorite	2	3	1	3	2	1
smectite	1	1	2	1	1	1
kaolinite	2	2		3	2	2
Pyrite	0.1	0.2	0.1	0.1		0.1
Gypsum	0.01	0.3	0.04	0.8	0.1	0.1
Jarosite	1	0.01			1	1
Othoclase	18	16	20	17	14	16
Quartz	45	43	46	40	48	48
QSP	65	85	70	55	70	70
Argilic	5		10			
Intrusive	99					
Amalia	1		99	10	10	100
Andesite		100	2	90	90	
Proplytic		2		7		
QMWI	7	2	7	7	7	7

APPENDIX 4. Summary description of the debris flow profile and comparison of Questa materials.

TABLE 4-1. Description of the debris flow profile samples.

Depth interval (ft)	Grain Size	Color	Grain angularity	Sedimentary structure	Description	Cementation	Sample collected
2	Boulders to clay	Brown	Angular	massive	Well graded	Moderate	MIN-GFA-0001
3	Boulder to clay	Brown	Angular	massive	Well graded	moderate	MIN-GFA-0003

Depth interval (ft)	Grain Size	Color	Grain angularity	Sedimentary structure	Description	Cementation	Sample collected
6.4	Boulder to clay	brown	Angular	Massive	Well graded	strong	MIN-GFA-0005
12	Gravel to fine silt	Brown	Angular	massive	Poorly graded gravel	strong	MIN-GFA-0006
13	Cobble to fine silt		Angular to subangular	massive	Poorly graded gravel	moderate	MIN-GFA-0007
27	Coarse gravel to sandy	Light reddish brown	Angular to subangular	Massive		Well	MIN-GFA-0009

TABLE 4-2. Comparison of the different weathering environments in the rock piles and analog sites in the Questa area. QSP=quartz-sericite-pyrite. See McLemore et al. (2008b) for more details.

Feature	Rock Pile	Alteration Scar	Debris Flow	Colluvium/ weathered bedrock
Rock types	Andesite Rhyolite Aplite Porphyry Intrusion	Andesite Rhyolite Aplite Porphyry Intrusion	Andesite Rhyolite Aplite Porphyry Intrusion	Andesite Rhyolite
Unified soil classification	GP-GC, GC, GP-GM, GW, GW-GC, SP-SC, SC, SW-SC, SM	GP-GC, GP	GP, SP, GP-GC	GP-GC, GP
% fines	0.2-46 Mean 7.5 Std Dev. 6 No of Samples=89	0.6-20 Mean 5.2 Std Dev. 4 No of Samples=18	0.3-6 Mean 1.8 Std Dev. 2 No of Samples=12	3-40 Mean 20 Std Dev. 11 No of Samples=30
Water content (%)	1-24 Mean 10 Std Dev. 4 No of Samples=390	1-20 Mean 9 Std Dev. 4 No of Samples=48	1-29 Mean 5 Std Dev. 4 No of Samples=36	9-26 Mean 14 Std Dev. 3 No of Samples=13
Paste pH	1.6-11.2 Mean 4.9 std dev 1.9 No of samples 1534	2.0-6.7 Mean 3.4 std dev 1.1 No of samples 84	2.0-6.9 Mean 4.5 std dev 1.3 No of samples 58	2.4-8.6 Mean 3.8 std dev 1.3 No of samples 45
Pyrite content (%)	Low to high 0-14% (mean 1.0%; std dev. 1.2%, No of samples=1098)	Low to high 0-11% (mean 0.7%, std dev 1.8%, No of samples=62)	Low to medium 0-0.2% (mean 0.03%, std dev 0.06%, No of samples=22)	Low to high 0-5.1% (mean 0.4%, std dev 1.1%, No of samples 26)
Dry density kg/m^3	1200-3100 Mean 1800 Std Dev. 200 No of Samples=320	1500-2300 Mean 1900 Std Dev. 210 No of Samples=13	1300-2500 Mean 1900 Std Dev. 380 No of Samples=11	2200-3200 Mean 2700 No of Samples=2
Particle shape	Angular to subangular to subrounded	Subangular	Subangular to subrounded	Subangular to subrounded
Plasticity Index (%)	0.2-20 Mean 10 Std Dev. 5 No of Samples=134	5-25 Mean 12 Std Dev. 5 No of Samples=30	3-14 Mean 7 Std Dev. 3 No of Samples=18	5-23 Mean 13 Std Dev. 5 No of Samples=17
Degree of chemical cementation (visual observation)	Low to moderate (sulfates, Fe oxides)	Moderate to high (sulfates, Fe oxides)	Moderate to high (sulfates, Fe oxides)	Moderate to high (sulfates, Fe oxides)
Slake durability index (%)	80.9-99.5 Mean 96.6 Std Dev. 3.1 No of Samples 120	64.5-98.5 Mean 89.2 Std Dev. 9.2 No of Samples 24	96.1-99.6 Mean 98.4 Std Dev. 0.9 No of Samples 18	93-98.5 Mean 95.7 Std Dev. 1.7 No. of Samples = 9
Point Load index (MPa)	0.6-8.2 Mean 3.8 Std Dev. 1.7 No of Samples 59	1.7-3.8 Mean 2.8 Std Dev. 0.8 No of Samples 4	2.6-6 Mean 4 Std Dev. 1 No of Samples 12	Not determined
Peak friction angle (degrees), 2-inch shear box (NMT data)	35.3-50.3 Mean 42 Std Dev. 3 No of Samples=101	33.4-54.3 Mean 41 Std Dev. 5 No of Samples=22	39.2-50.1 Mean 44 Std Dev. 4 No of Samples=12	36.9-45.8 Mean 42 Std Dev. 3 No of Samples=41
Average cohesion (kPa), in-situ shear tests	0-25.9 Mean 9.6 Std dev 7.3 No of samples=20	12.1-23.9 Mean 18.1 No of samples=2	31.4-46.1 Mean 38.8 No of samples=2	Not determined